Neuronal T-type α1H Calcium Channels Induce Neuritogenesis and Expression of High-Voltage-Activated Calcium Channels in the NG108–15 Cell Line

Jean Chemin, Joël Nargeot, and Philippe Lory

Institut de Génétique Humaine, Centre National de la Recherche Scientifique, Unité Propre de Recherche 1142, F-34396 Montpellier cedex 05, France

Neuronal differentiation involves both morphological and electrophysiological changes, which depend on calcium influx. Voltage-gated calcium channels (VGCCs) represent a major route for calcium entry into neurons. The recently cloned low-voltage-activated T-type calcium channels (T-channels) are the first class of VGCCs functionally expressed in most developing neurons, as well as in neuroblastoma cell lines, but their roles in neuronal development are yet unknown. Here, we document the part played by T-channels in neuronal differentiation. Using NG108–15, a cell line that recapitulates early steps of neuronal differentiation, we demonstrate that blocking T-currents by nickel, mibefradil, or the endogenous cannabinoid anandamide prevents neuritogenesis without affecting neurite outgrowth. Similar results were obtained using antisense oligodeoxynucleotides directed against the α1H T-channel subunit. Furthermore, we describe that inhibition of α1H T-channel activity impairs concomitantly, but independently, both high-voltage-activated calcium channel expression and neuritogenesis, providing strong evidence for a dual role of T-channels in both morphological and electrical changes at early stages of neuronal differentiation.

Key words: T-type calcium channel; differentiation; neuritogenesis; HVA calcium channel; neuroblastoma NG108–15 cell line; antisense

Neuroblast differentiation into neurons is associated with morphological and electrical changes. Major morphological changes are the appearance of axonal and dendritic extensions, collectively called neurites. The electrical changes mainly result from the expression of various voltage-gated channels, and many studies have indicated a correlation between calcium current expression and morphological differentiation (Bader et al., 1983). Voltage-gated calcium channels constitute a central component of signal transduction cascades (Berridge, 1998), and neuronal differentiation is altered when calcium influx is inhibited (Gu and Spitzer, 1997). In most neurons, including hippocampal, motor, and sensory neurons, low-voltage-activated T-type calcium currents (T-currents) appear first, whereas high-voltage-activated (HVA) calcium currents (especially L- and N-types) appear later in conjunction with neurite extension and dominate the total calcium influx in mature neurons (Nowycky et al., 1985; Yaari et al., 1987; Gottmann et al., 1988; McCobb et al.,1989). This sequence of events is also observed in a variety of neuroblastoma cell lines, including NG108–15 cells (Nirenberg et al., 1983; Hamprecht et al., 1985; Docherty et al., 1991).

Although the presence of T-currents at early stages of neuronal development suggests that they are involved in neuronal differentiation (Frischknecht and Randall, 1998), the functional significance of their early expression in neuroblasts remains to be determined. Cellular models that recapitulate early steps of neuronal differentiation allow such an investigation in a more defined way than *in vitro* cultures of undifferentiated neuroblasts collected from early embryos, which cannot be manipulated as a homogenous–synchronized cell population. It has been demonstrated that the neuroblastoma–glioma NG108–15 cell line, which expresses classical T-type calcium channels (Randall and Tsien, 1997), is a suitable model for investigating the mechanisms involved in neuronal development and differentiation, especially for the transition from neuroblast to neuron (Nirenberg et al., 1983; Hamprecht et al., 1985; Docherty et al., 1991). NG108–15 cells display a synchronized neuronal differentiation when cultivated in the presence of cAMP (Nirenberg et al., 1983), and differentiated NG108–15 cells exhibit well characterized morphological, electrophysiological, and pharmacological properties that are similar to neurons, including neurite outgrowth, synapse formation, and HVA calcium channel expression (Kleinman et al., 1988; Han et al., 1991; Kasai and Neher, 1992; Taussig et al., 1992). Using this cellular model, we describe in the present study that inhibition of T-channel activity impairs concomitantly, but independently, HVA channel expression and neuritogenesis, indicating a crucial role of T-channels encoded by the α1H subunit in both morphological and electrical changes during early stage of neuronal differentiation.

Received Jan. 7, 2002; revised May 10, 2002; accepted May 17, 2002.

This work was supported by Centre National de la Recherche Scientifique, the Association pour la Recherche contre le Cancer, and the Ligue contre le Cancer. We thank Drs. M. Mangoni, E. Bourinet, C. Altier, S. Barrère, D. Fisher, S. Jarvis, and S. Dubel for helpful discussions and comments on this manuscript. We are grateful to Dr. F. A. Rassendren for technical help with Southern blot techniques, Dr. G. Dayanithi (Institut National de la Santé et de la Recherche Médicale U432) for the gift of SNX-482, and Dr. I. A. Lefevre for critical reading of this manuscript.

Correspondence should be addressed to Philippe Lory, Institut de Génétique Humaine, Centre National de la Recherche Scientifique, Unité Propre de Recherche 1142, 141 rue de la Cardonille, F-34396 Montpellier cedex 05, France. E-mail: philippe.lory@igh.cnrs.fr.

MATERIALS AND METHODS

Cell culture and assessment of neurite outgrowth. The NG108–15 cell line was used between 15 and 40 passages and was cultured as described previously (Chemin et al., 2001b). Cells were seeded at 250 cells/mm^2 in 35 mm Petri dishes, and differentiation was induced by decreasing fetal calf serum (Eurobio, Les Ulis, France) in the medium to 1% and by adding 1 mM dibutyryl cAMP (Sigma, St. Louis, MO). Fourteen hours

Table 1. Normalized ratio of the number of cells expressing neurites with respect to neurite length

	O-		O–		O——	
Control	1 (57 ± 2%; $n = 27$)		1 (21 ± 1%; $n = 27$)		1 (21 ± 2%; $n = 27$)	
30 μM Ni^{2+}	0.93 ± 0.04 (16)	NS	1.07 ± 0.06 (16)	NS	1.16 ± 0.12 (16)	NS
AS-α1H	1.03 ± 0.05 (16)	NS	0.92 ± 0.09 (16)	NS	1.06 ± 0.13 (16)	NS
Without cAMP	1.45 ± 0.04 (10)	***	0.51 ± 0.06 (10)	***	0.27 ± 0.05 (10)	***

No effect of the block of T-currents on the neurite length. Neurite extension was evaluated by counting cells with short neurites (process length, ≤1 cell body diameter), medium-sized neurites (process length, >1 cell body diameter and <2 cell body diameter), and long neurites (process length, >2 cell body diameter). The values represent the ratio of the number of cells expressing neurites with respect to neurite length normalized according to control experiments. Values are expressed as mean ± SEM and n values are the number of independent experiments for which at least 100 cells per dish on three different dishes were counted. NS, Not significant; ***$p < 0.001$.

after plating, cells were examined under the microscope, and multiple random fields were examined. Neurite formation was quantified by scoring the percentage of cells possessing neurites over the total number of cells. Neurite extension (Table 1) was evaluated by counting cells with short neurites (length, ≤1 cell body diameter), medium-sized neurites (length, >1 cell body diameter and <2 cell body diameter), and long neurites (length, >2 cell body diameter). Cell clumps containing more than five cells were not considered in the counting. These experiments were conducted using a double-blind strategy to avoid errors attributable to subjective judgment. Dunnett's multiple comparison test was used for statistical comparisons, and the values were expressed as mean ± SEM of n independent experiments.

Whole-cell patch-clamp recordings. Macroscopic currents were recorded by the whole-cell patch-clamp technique at room temperature using an Axopatch 200B amplifier (Axon Instruments, Foster City, CA). Data were acquired on a personal computer using the pClamp6 software suite (Axon Instruments). Current recordings were filtered at 5 kHz. Capacitance and R_s were compensated by 85–95% using the whole-cell parameters of the Axopatch 200B amplifier. The extracellular solution contained (in mM): 2 $CaCl_2$, 160 tetraethylammonium (TEA)-Cl, and 10 HEPES, pH 7.4 with TEA-OH. Pipettes made of borosilicate glass had a typical resistance of 1–3 MΩ when filled with a solution containing (in mM): 110 CsCl, 10 EGTA, 10 HEPES, 3 Mg-ATP, and 0.6 Na-GTP, pH 7.2 with CsOH. Whole-cell currents were analyzed as described previously (Chemin et al., 2001a), and Student's t tests or one-way ANOVA combined with a Student–Newman–Keuls *post hoc* test (for multiple comparisons) were used and considered significant with *$p < 0.05$, **$p < 0.01$, and ***$p < 0.001$ as indicated in the table and in figures. Results are presented as the mean ± SEM, and n is the number of cells used.

Bromodeoxyuridine labeling. For bromodeoxyuridine (BrdU) labeling, cells were plated at 250 cells/mm^2 on 12 mm glass coverslips. After 3 hr, 10 μM BrdU (Roche Products, Hertforshire, UK) was added to the medium for 45 min. BrdU-treated cells were rinsed with PBS and fixed at room temperature for 10 min in a 3.7% paraformaldehyde solution (Sigma). Immunostainings and Hoechst 33258 nuclear dye (Sigma) labeling were performed as described previously (Chemin et al., 2000). Control experiments were performed in the absence of BrdU incorporation (data not shown). Digital images were acquired on a microscope (Leica, Nussloch, Germany) and further analyzed using Adobe Photoshop 4.0 (Adobe Systems, San Jose, CA). Percentage of proliferative cells was defined as the ratio of BrdU-positive cells over Hoechst-labeled cells (using multiple random microscope fields). One-way ANOVA combined with a Student–Newman–Keuls *post hoc* test were used to compare the different values and were considered significant at $p < 0.05$. The values were expressed as mean ± SEM, and n is the number of independent experiments.

Reverse transcription-PCR and Southern blotting. RNA from undifferentiated and differentiated NG108–15 cells, as well as from rat and mouse brains, were isolated using Trizol (Invitrogen, Gaithersburg, MD) according to the protocol of the manufacturer. Poly(A^+) RNA was separated using an mRNA purification kit (Dynal, Great Neck, NY). Reverse transcription (RT) was performed with superscript II reverse transcriptase primed with random hexamers using the superscript first-strand synthesis system for RT-PCR (Invitrogen). PCR primers were designed for the analysis of the three T-channel α_1 subunits. The α1G primers 5′-GCTCTTTACTTCATCGCCCTC-3′ (forward) and 5′-CCTCATCATTGTCATCATCCCC-3′ (reverse) generated a 795 bp fragment. The α1H primers 5′-GGACGGACACAACGTGAG-3′ (forward) and 5′-GTTCCAGTTGATGCAGGC-3′ (reverse) generated a 459 bp fragment. The α1I primers 5′-ATGCTGGTGATCCTGCTGAAC-3′ (forward) and 5′-GCACGCGGTTGATGGCTTTGAG-3′ (reverse) generated a 300 bp fragment. Southern blotting was performed using standard methods (Sambrook et al., 1989). Briefly, 10 pmol of oligonucleotides matching an internal sequence of each PCR product (α1G, 5′-GCCAAGAGTTCCTTTGACCT-3′; α1H, 5′-GGAACAACAACCTGACCTTC-3′; and α1I, 5′-TGCAAGATCCTGCAGGTCTT-3′) were labeled with [γ-^{32}P]ATP using T_4 polynucleotide kinase. Membranes were hybridized in Express-Hyb buffer (Clontech, Cambridge, UK) overnight (42°C) and further revealed by autoradiography. Negative controls for RT-PCR were obtained using reverse transcriptase reaction of mRNA samples in which random hexamers were omitted (negative RT; see Fig. 2), and positive controls were made using mRNA obtained from rat brain, as well as from mouse brain.

Transfection protocols. Antisense (AS) oligodeoxynucleotides against α1G mRNA [5′-CCTCATCATTGTCATCATCC-3′ (AS-α1G)], AS against α1H subunit mRNA [5′-GTTCCAGTTGATGCAGGC-3′ (AS-α1H)], and AS against α1I subunit mRNA [5′-GCACGCGGTTGATGGCTTTG-3′ (AS-α1I)] were used in transfection experiments. A scramble oligodeoxynucleotide 5′-GTAGCATGATCGGTGCTC-3′ (*Scramble* in figure legends) was used as control. Two hours before transfection, cells were plated at ~50% confluence in 35 mm Petri dishes. A standard transfection procedure was performed using Fugene 6 transfection reagent (Roche Products) with 500 nM/dish of AS solution. Three days later, cells were plated at 250 cells/mm^2 in 35 mm Petri dishes, and differentiation was induced as described above.

RESULTS

Calcium currents in undifferentiated and differentiated NG108–15 cells

In undifferentiated conditions, NG108–15 cells were preferentially organized in clusters and displayed no neurite extension (Fig. 1*A*). In this condition, T-type calcium currents were observed in 95% of the cells (T-current density, 1.5 ± 0.3 pA/pF; $n = 40$ cells) (Fig. 1*C*,*E*), whereas HVA currents were mostly absent or very weak (HVA current density, 0.22 ± 0.11 pA/pF; $n = 40$ cells). Three to 6 d after differentiation, cells exhibited neurites (Fig. 1*B*), and, consequently, membrane capacitance was larger [53.7 ± 4.3 pF ($n = 40$ cells) and 91.3 ± 12.1 pF ($n = 30$ cells) for undifferentiated and differentiated cells, respectively]. After differentiation, the total calcium current density was significantly increased because of the expression of HVA currents (HVA current density, 4.9 ± 0.9 pA/pF; $n = 30$ cells) (Fig. 1*D*,*F*). In differentiated cells, the HVA current composition was evaluated using specific pharmacological agents (Fig. 1*F*, *inset*). Calcium currents were strongly sensitive to ω-conotoxin-GVIA (percentage of block, 43 ± 9%; $n = 12$ cells) and to nitrendipine (percentage of block, 34 ± 7%; $n = 12$ cells), which block N- and L-type currents, respectively. A smaller fraction of the calcium current was blocked by ω-agatoxin-IVB, a blocker of P/Q channels (percentage of block, 11 ± 4%; $n = 12$ cells). Also, a fraction of this current (R-type, 12 ± 7%; $n = 12$ cells) was insensitive to all of the previously described blockers, as well as to 30 μM nickel and SNX-482 (Newcomb et al., 1998). In contrast, no change in

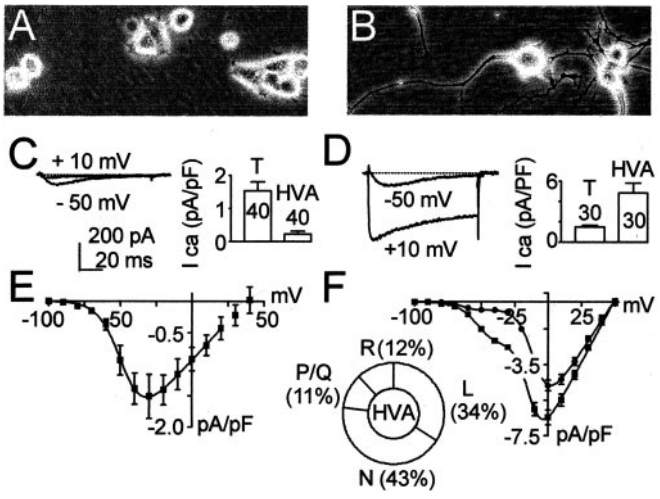

Figure 1. Properties of calcium currents in undifferentiated and differentiated NG108–15 cells. *A*, Representative phase-contrast image of undifferentiated NG108–15 cells. *B*, Representative phase-contrast image of NG108–15 cells displaying long neurites 6 d after differentiation. *C*, *D*, Typical traces of calcium currents and average current density of T-currents and HVA currents recorded in undifferentiated (*C*) and differentiated (*D*) NG108–15 cells. To avoid any contamination of T-currents by HVA currents and vice versa, T-currents were measured as the peak current at −50 mV (approximately two-thirds of the maximum T-current amplitude), whereas HVA currents were measured at +10 mV, 100 msec after the beginning of the test pulse, i.e., after complete inactivation of T-currents. *E*, Current–voltage relationship of calcium current in undifferentiated NG108–15 cells ($n = 30$ cells). *F*, Current–voltage relationship of calcium current measured at the peak (sum of T-currents and HVA currents; *squares*) and 100 msec after the beginning of the test pulse (HVA currents; *circles*) in differentiated NG108–15 cells ($n = 20$ cells). In all of these experiments, holding potential (HP) was −110 mV, and Ca^{2+} (2 mM) was used as charge carrier. *F*, *Inset*, Composition of the HVA calcium current component (presented as percentage of the total HVA current) in differentiated cells was determined by the use of specific blockers. Currents were measured at +10 mV from a HP of −60 mV, and 2 μM nitrendipine (L-type blockade), 1 μM ω-conotoxin-GVIA (N-type blockade), and 200 nM agatoxin-IVB (P/Q-type blockade) were applied in this order ($n = 12$ cells). A fraction of calcium current (R-type) was insensitive to all previous blockers, as well as to 30 μM nickel and 200 nM SNX-482.

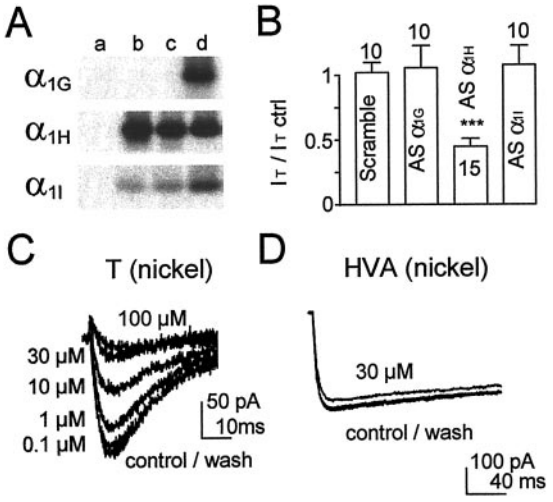

Figure 2. *A*, Molecular identification of T-channel subunits expressed in NG108–15 cells as determined by Southern blotting of RT-PCR reactions for α1G, α1H, and α1I subunit mRNAs. The conditions tested are negative RT (*a*) (see Materials and Methods), undifferentiated NG108–15 cells (*b*), differentiated NG108–15 cells (*c*), and rat brain (*d*). *B*, Effects of specific antisense oligodeoxynucleotides against T-channel subunit mRNAs on T-currents measured at −50 mV in undifferentiated cells. *C*, *D*, Effects of increasing concentrations of Ni^{2+} on T-currents (*C*) and effects of 30 μM Ni^{2+} on HVA currents (*D*) in differentiated NG108–15 cells. T-currents were recorded at −50 mV from an HP of −110 mV, whereas HVA currents were recorded at +10 mV from an HP of −60 mV.

T-current density was observed after differentiation (1.5 ± 0.2 pA/pF; $n = 30$ cells), and the electrophysiological properties of T-currents were similar in undifferentiated and differentiated cells (data not shown), suggesting that differentiation does not affect T-channel expression in NG108–15 cells.

Molecular characterization of the α1H nickel-sensitive T-currents

To resolve the molecular nature of the T-channels expressed in NG108–15 cells, we performed RT-PCR experiments followed by Southern blotting analysis (see Materials and Methods). A strong RT-PCR signal for the α1H subunit mRNA was found in both undifferentiated and differentiated NG108–15 cells, whereas no α1G and only small amounts of α1I mRNA were detected (Fig. 2*A*). AS oligodeoxynucleotides were designed against each T-channel subunit mRNA to knock-down T-channel expression. The percentage of transfection was ~70%, as measured with AS coupled to FITC. AS-α1H significantly decreased the T-current amplitude in undifferentiated ($I/I_{control}$, 0.45 ± 0.06; $n = 15$ cells) as well as in differentiated NG108–15 cells ($I/I_{control}$, 0.4 ± 0.1; $n = 12$ cells; data not shown), whereas AS-α1G, AS-α1I, and a scramble AS had no effect (Fig. 2*B*). Moreover, we observed no difference in the electrophysiological characteristics between the residual T-currents after AS-α1H transfection and the control T-currents, including steady-state activation and inactivation properties and activation and inactivation kinetics (data not shown), further indicating that only α1H channels are functionally expressed in NG108–15 cells. In addition, micromolar concentrations of nickel ions (Ni^{2+}) inhibited T-currents in undifferentiated and differentiated NG108–15 cells [IC_{50}, 4.1 ± 0.2 μM ($n = 20$ cells) and 3.8 ± 0.4 μM ($n = 20$ cells), respectively] (Fig. 2*C*). For a concentration of 30 μM Ni^{2+} that completely blocked T-currents (percentage of block, 96 ± 1%; $n = 20$ cells), HVA currents were only weakly affected (percentage of block, 12 ± 4%; $n = 20$ cells), even after 30 min of Ni^{2+} perfusion, and this inhibition was fully reversible (Fig. 2*D*).

T-Currents promote differentiation and neuritogenesis

We next investigated whether T-currents could promote neuritogenesis and neurite extension. After only 14 hr in differentiating conditions, we observed a very large increase in the number of cells displaying neurites [from 6.2 ± 0.6% ($n = 8$ experiments) to 65 ± 2% ($n = 30$ experiments), for undifferentiated and differentiated cells, respectively]. In contrast, differentiation occurring in the presence of 30 μM Ni^{2+} dramatically reduced neuritogenesis. Figure 3 shows that treatment with the T-channel blockers Ni^{2+} and mibefradil significantly decreased the number of cells with neurites [percentage of cells with neurites/control, 65 ± 2% ($n = 20$ experiments) and 78 ± 3% ($n = 15$ experiments), respectively], whereas HVA blockers had no effect. Similarly, 1 μM methanandamide, the nonhydrolyzable analog of the endocannabinoid anandamide, recently identified as an endogenous cannabinoid (CB) receptor ligand that also directly inhibits T-currents (Chemin et al., 2001c), decreased the number of cells with neurites in the presence of 100 nM of the CB1 receptor

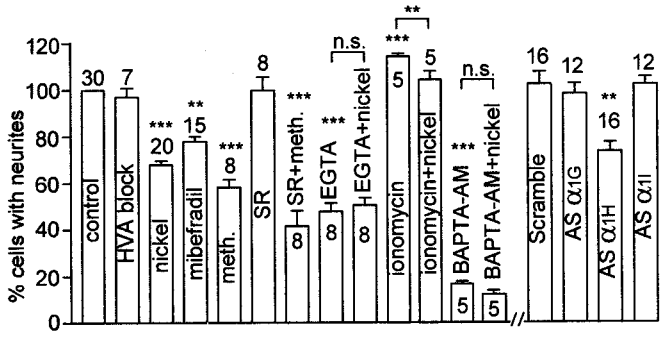

Figure 3. Block of T-currents decreases neuritogenesis in NG108–15 cells. Cell analysis was performed 14 hr after inducing differentiation. Effects of various calcium channel blockers (*left*) and specific AS oligodeoxynucleotides against the T-type channel subunit mRNAs (*right*) on the percentage of cells exhibiting neurites. Inhibition of HVA currents was performed using a mix of nitrendipine (2 μM), ω-conotoxin-GVIA (1 μM), and ω-agatoxin-IVB (200 nM). Inhibition of T-currents was performed using Ni^{2+} (30 μM), mibefradil (1 μM), and methanandamide (*meth*; 1 μM) in the presence or absence of the CB1 receptor antagonist SR141716A (*SR*; 100 nM). EGTA was used at 1.5 mM, which reduced free external Ca^{2+} to ~300 μM. BAPTA-AM and ionomycin were used at 10 μM and 100 nM, respectively. Results are normalized with respect to the percentage of cells expressing neurites in the corresponding control culture condition. The *n* values above each *bar* correspond to independent experiments for which at least 100 cells per dish on three different dishes were counted.

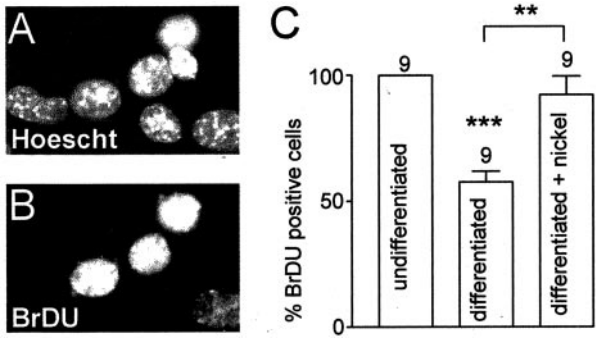

Figure 4. Block of T-currents (30 μM Ni^{2+} incubation) increases the percentage of BrdU-positive cells (S-phase labeling) 4 hr after inducing differentiation. Example of Hoechst 33258 (*A*) and BrdU (*B*) labeling in undifferentiated cells. *C*, Compared with differentiated cells, 30 μM Ni^{2+} prevented loss of BrdU incorporation. Results are normalized according to the percentage of BrdU-positive NG108–15 cells in the undifferentiated condition, and *n* values correspond to independent experiments for which at least 100 cells per dish on three different dishes were counted.

antagonist SR141716A (percentage of cells with neurites/control, 41 ± 6%; $n = 8$ experiments). Reducing free external Ca^{2+} with EGTA (see figure legend) inhibited neuritogenesis (percentage of cells with neurites/control, 45 ± 5%; $n = 8$ experiments), and no additional effect of Ni^{2+} was observed in these conditions (Fig. 3). Similarly, reducing free internal Ca^{2+} with 10 μM BAPTA-AM inhibited neuritogenesis (percentage of cells with neurites/control, 17 ± 1%; $n = 5$ experiments), and no additional effect of Ni^{2+} was observed in these conditions (Fig. 3). Conversely, increasing free internal Ca^{2+} with 100 nM ionomycin increased neuritogenesis (percentage of cells with neurites/control, 115 ± 1%; $n = 5$ experiments). In this later case, it is worth noting that Ni^{2+} inhibited significantly neuritogenesis (Fig. 3). Finally, AS-α1H specifically decreased the number of cells exhibiting neurites (percentage of cells with neurites/control, 74 ± 4%; $n = 16$ experiments) (Fig. 3). Interestingly, neither AS-α1H nor Ni^{2+} affected neurite length (Table 1), suggesting that T-currents are important for initiation of neuritogenesis but are not involved in neurite extension. In contrast, removing cAMP from the differentiating medium affected neuritogenesis (percentage of cells with neurites/control, 60 ± 10%; $n = 8$ experiments; data not shown), as well as neurite extension (Table 1).

Considering that α1H T-currents appear to have an early role in NG108–15 differentiation, we also explored whether T-currents could control the proliferation of NG108–15 cells after 4 hr of differentiation. For this purpose, we performed labeling with BrdU, a thymidine analog that is incorporated specifically into cells in S-phase (Fig. 4). After 4 hr of differentiation, the percentage of BrdU-positive cells decreased (percentage of positive cells/undifferentiated cells, 57 ± 4%; $n = 9$ experiments), indicating that differentiation was initiated. In contrast, in the presence of 30 μM Ni^{2+}, cell proliferation was not significantly reduced compared with undifferentiated cells (percentage of positive cells/undifferentiated cells, 92 ± 7%; $n = 9$ experiments). Overall, these data suggest an important role of T-currents in triggering the onset of differentiation, leading to morphological changes.

Block of T-currents promotes inhibition of HVA calcium current expression

We next investigated whether T-currents could also contribute to changes in the expression of HVA calcium channels, a hallmark of neuronal differentiation. Interestingly, a strong correlation between HVA and T-current densities was observed ($r = 0.8$; $p < 0.001$; $n = 80$ cells) (Fig. 5*A*), suggesting that T-currents may regulate expression of HVA channels. The correlation between HVA and T-current densities was abolished with 30 μM Ni^{2+} treatment during differentiation ($r = 0.14$; $p > 0.05$; $n = 50$ cells) (Fig. 5*B*). In this case (Fig. 5*C*,*D*), a significant decrease in HVA currents was observed, because HVA current density was 5.1 ± 1.9 pA/pF ($n = 20$ cells) in control cells and 1.1 ± 0.3 pA/pF ($n = 28$ cells) in Ni^{2+}-treated cells after Ni^{2+} washout ($p < 0.001$). In addition, we observed no change in the pharmacological properties of the HVA current after Ni^{2+} treatment ($n = 15$ cells; data not shown), suggesting that functional expression of each type of HVA channels was similarly inhibited. In contrast, T-current density was not affected by chronic Ni^{2+} treatment [1.21 ± 0.22 pA/pF ($n = 20$ cells) and 1.12 ± 0.38 pA/pF ($n = 28$ cells) for control and Ni^{2+}-treated cells, respectively] (Fig. 5*C*), indicating that inhibition of HVA currents was not attributable to inadequate removal of Ni^{2+} ions from the medium. More importantly, transfection of AS-α1H significantly decreased HVA currents (HVA current density/control, 0.36 ± 0.16 pA/pF; $n = 12$ cells), similar to chronic Ni^{2+} treatment (Fig. 5*D*). Because the inhibition of HVA current expression could be a consequence of the decrease in the number of cells displaying neurites, we next analyzed HVA current expression with respect to the neurite length. Chronic Ni^{2+} treatment decreased neuritogenesis without affecting neurite extension, and ~45% of the cells displayed long neurites after 4–6 d of differentiation. In control cells, HVA current density increased with the neurite length [HVA current density, 0.9 ± 0.4 pA/pF ($n = 10$ cells) and 9.2 ± 2.9 pA/pF ($n = 10$ cells) in cells with short and long neurites, respectively] (Fig. 5*E*), whereas T-current density did not [1.5 ± 0.3 pA/pF ($n = 10$ cells) in cells with short neurites and 1.4 ± 0.3 pA/pF ($n = 10$ cells) in cells with long neurites; data not shown]. In contrast, no enhancement of HVA currents was observed in Ni^{2+}-treated

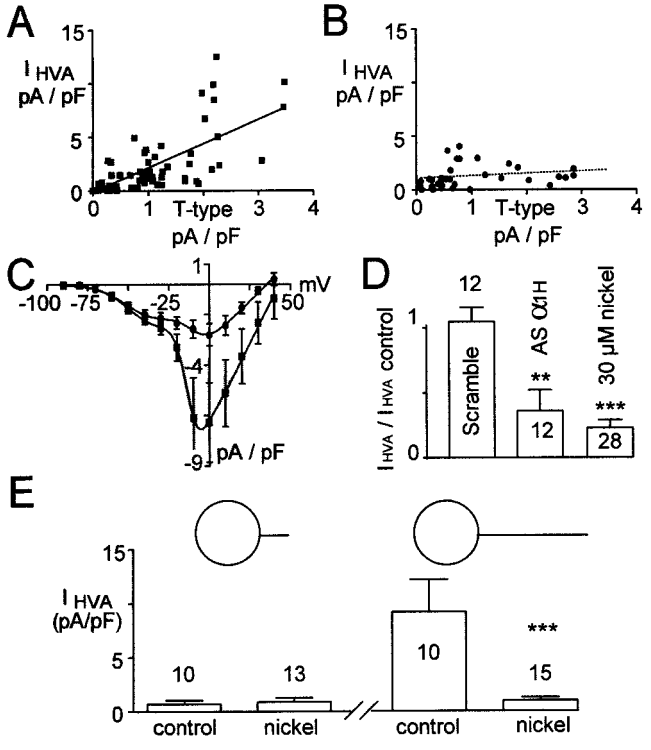

Figure 5. Block of T-currents decreases HVA current expression 4 d after the induction of differentiation. *A*, *B*, Correlation between HVA and T-current densities (*A*), which was abolished after chronic 30 μM Ni^{2+} treatment during differentiation (*B*). For electrophysiological recordings, cells were rinsed for at least 2 hr with control differentiated medium to wash out external Ni^{2+} ions before Ca^{2+} current measurements. *C*, Effects of chronic Ni^{2+} treatment on current–voltage relationship for Ca^{2+} currents (*circles*) compared with current–voltage relationship for Ca^{2+} currents in control cells (*squares*). *D*, Transfection of NG108–15 cells with antisense oligodeoxynucleotide against the α1H subunit mRNA (AS-α1H) decreased HVA currents similarly to chronic treatment with 30 μM Ni^{2+}. *E*, In cultures treated with Ni^{2+}, there was no change in HVA current expression in cells with short neurites (process length, ≤1 cell body diameter), whereas HVA currents were absent in cells expressing long neurites (process length, >2 cell body diameter) compared with control cultures.

cells [HVA current density, 1.1 ± 0.3 pA/pF (n = 15 cells) and 1.2 ± 0.5 pA/pF (n = 13 cells) in cells with short and long neurites, respectively] (Fig. 5*E*). Altogether, these data demonstrate that T-currents are important for the expression of HVA calcium conductances independently from the induction of neuritogenesis.

DISCUSSION

T-type channels are the first voltage-gated calcium channels expressed in developing neurons. Although it is widely admitted that calcium influx plays a crucial role in neuronal differentiation, the role of T-channels in this process is unknown. Using the neuronal model NG108–15 cell line, we provide new findings indicating that T-currents encoded by the α1H subunit contribute to morphological and electrical changes occurring during neuronal differentiation. We report that T-currents are involved in the onset of the differentiation process, leading to the arrest of cell proliferation and the induction of neuritogenesis. In addition, the data reveal that T-currents are involved in the expression of HVA calcium currents, indicating a crucial role of T-channels in neuronal differentiation.

Our study demonstrates that NG108–15 cells exhibit both low-voltage-activated T-currents and HVA currents and that these two classes of channels are differentially modulated during neuronal differentiation. Undifferentiated NG108–15 cells have no neurites and display calcium currents of small amplitude that are entirely T-currents. Differentiation of NG108–15 cells affected neither the density nor the electrophysiological and pharmacological properties of T-currents. In contrast, we found a striking change in the functional expression of HVA currents during differentiation, which is in agreement with previous studies (Freedman et al., 1984; Kasai and Neher, 1992; Lukyanetz, 1998). The increase in HVA current expression in differentiating NG108–15 cells occurs in concert with neuritogenesis, similar to that observed in many neurons (Nowycky et al., 1985; Yaari et al., 1987; Gottmann et al., 1988; McCobb et al.,1989). The presence of T-currents in both undifferentiated NG108–15 cells and every cell with neurites designates T-channels as potential actors in neuronal differentiation. The recent characterization of three genes coding for T-type α1 subunits [α1G ($Ca_V3.1$), α1H ($Ca_V3.2$), and α1I ($Ca_V3.3$)] (Cribbs et al., 1998; Perez-Reyes et al., 1998; Klugbauer et al., 1999; Lee et al. 1999a; Williams et al., 1999; Monteil et al., 2000a,b; McRory et al., 2001) has enabled the molecular investigation of T-channel functions. Both in undifferentiated and differentiated NG108–15 cells, T-currents are very sensitive to Ni^{2+} and have characteristics similar to those described in neurons (Carbone and Lux, 1984; Armstrong and Matteson, 1985; Nowycky et al., 1985; Fox et al., 1987; Randall and Tsien, 1997). Overall, RT-PCR experiments and Ni^{2+} sensitivity of T-currents (Lee et al., 1999b) both indicate that these channels in NG108–15 cells comprise the α1H subunit. The use of pharmacological agents and antisense strategies allowed us to demonstrate that α1H T-currents contribute to morphological and electrical changes during neuronal differentiation. During differentiation, NG108–15 cells rapidly lose their ability to proliferate, and this can be prevented if α1H T-currents are blocked. More importantly, blockade of T-current decreases the number of cells expressing neurites. Such a reduction in neuritogenesis depends on the Ca^{2+} influx and is observed with a variety of T-channel blockers, including anandamide, which directly block T-currents independently of CB receptors (Chemin et al., 2001c). Interestingly, our data indicate that there is no correlation between neurite length and T-current density and that the block of T-currents does not affect neurite outgrowth. Because appearance of HVA currents and neuritogenesis are concomitant (and possibly associated) events, T-channel blockade could also affect HVA channel expression. Indeed, we found a strong correlation between T-current and HVA current amplitudes, and the chronic block of T-currents inhibits expression of HVA currents. Nevertheless, inhibition of HVA current expression cannot simply be explained by the decrease in neuritogenesis because it is observed even in cells with long neurites. Conversely, inhibition of HVA current expression does not account for the inhibition of neuritogenesis because pharmacological blockade of HVA currents does not affect the number cells expressing neurites. Altogether, these data demonstrate that α1H T-currents play a central role in the early onset of morphological differentiation, as well as in the maturation of calcium conductances of the NG108–15 cell line.

Concluding remarks

To our knowledge, we are aware of no other study that either disproves or conclusively demonstrates a role played by T-channels in neuronal differentiation. NG108–15 is a cholinergic

cell line (Hamprecht et al., 1985; Docherty et al., 1991) in which T-current properties are similar to peripheral neurons (Carbone and Lux, 1984), which also express the α1H subunit (Talley et al., 1999). Two other cholinergic cell lines, SN56 (Kushmerick et al., 2001) and N1E-115 (Lievano et al., 1994), also exhibit Ni^{2+}-sensitive (α1H-related) T-currents that precede neuritogenesis and HVA channel expression, suggesting that α1H T-channels could play a specific role in neuronal differentiation of the cholinergic system. Ni^{2+}-sensitive T-currents are also present at early stages in the peripheral nervous system, including dorsal root ganglion neurons (Gottmann et al., 1988) and motor neurons (McCobb et al.,1989; Mynlieff and Beam, 1992). Similarly, dot blot analysis of human brain mRNA showed that the α1H subunit is expressed at higher level during fetal development (A. Monteil, P. Lory, and J. Nargeot, unpublished results), and Ni^{2+}-sensitive T-currents have been recorded in floor plate cells of the developing CNS (Frischknecht and Randall, 1998). Therefore, in the light of the results described here, the implication of α1H T-channels in neuronal differentiation should be analyzed in the peripheral nervous system, as well as in the CNS, in regions such as the hippocampus (Yaari et al., 1987). Ni^{2+}-sensitive α1H T-channels are likely to mediate differentiation of a variety of cell types, because it was shown recently that α1H T-channels promote differentiation (fusion) of human myoblasts (Bijlenga et al., 2000). In addition, in the human prostate cancer epithelial LNCaP cells, there is an elevated expression of α1H T-channels during cell differentiation, which is likely to facilitate neurite-like lengthening (Mariot et al., 2002). An important question that now needs to be addressed is how α1H T-channels contribute to differentiation and HVA channel expression. For skeletal muscle differentiation, it has been shown that α1H T-window currents could increase resting intracellular Ca^{2+} in fusing myoblasts (Bijlenga et al., 2000), a property that was also found for recombinant α1H T-channels overexpressed in HEK293 cells (Chemin et al., 2000). Although our data demonstrate that entry of Ca^{2+} through T-channels plays a crucial role in neuronal differentiation, we did not find any significant difference in intracellular Ca^{2+} concentration when comparing NG108–15 cells treated or not with Ni^{2+} using the Ca^{2+} indicator fura-2 (data not shown). Interestingly, although a rise of intracellular calcium seems crucial for T-channel-induced neuritogenesis (as assessed by the use of BAPTA-AM and ionomycin), block of T-channels in ionomycin-treated cells still inhibited neurite emergence. These data might be explained by the presence, close to T-channels, of Ca^{2+} buffer proteins that are capable of selectively transducing this Ca^{2+} signal, thus allowing neuritogenesis. Calcineurin and calmodulin are involved in neuronal differentiation (Goshima et al., 1993; Chang et al., 1995; Lautermilch and Spitzer, 2000) and are highly expressed in NG108–15 cells (Komeima et al., 2000; Higashida et al., 2001). It will therefore be of great interest to examine whether Ca^{2+} influx via α1H T-channels can modulate differentiation processes through these pathways.

REFERENCES

Armstrong CM, Matteson DR (1985) Two distinct populations of calcium channels in a clonal line of pituitary cells. Science 227:65–67.

Bader CR, Bertrand D, Dupin E, Kato AC (1983) Development of electrical membrane properties in cultured avian neural crest. Nature 305:808–810.

Berridge MJ (1998) Neuronal calcium signaling. Neuron 21:13–26.

Bijlenga P, Liu JH, Espinos E, Haenggeli CA, Fisher-Lougheed J, Bader CR, Bernheim L (2000) T-type α_{1H} Ca^{2+} channels are involved in Ca^{2+} signaling during terminal differentiation (fusion) of human myoblasts. Proc Natl Acad Sci USA 97:7627–7632.

Carbone E, Lux HD (1984) A low voltage-activated, fully inactivating Ca channel in vertebrate sensory neurones. Nature 310:501–502.

Chang HY, Takei K, Sydor AM, Born T, Rusnak F, Jay DG (1995) Asymmetric retraction of growth cone filopodia following focal inactivation of calcineurin. Nature 376:686–690.

Chemin J, Monteil A, Briquaire C, Richard S, Perez-Reyes E, Nargeot J, Lory P (2000) Overexpression of T-type calcium channels in HEK-293 cells increases intracellular calcium without affecting cellular proliferation. FEBS Lett 478:166–172.

Chemin J, Monteil A, Bourinet E, Nargeot J, Lory P (2001a) Alternatively spliced α_{1G} ($Ca_V3.1$) intracellular loops promote specific T-type Ca^{2+} channel gating properties. Biophys J 80:1238–1250.

Chemin J, Monteil A, Dubel S, Nargeot J, Lory P (2001b) The α_{1I} T-type Ca^{2+} channel exhibits faster gating properties when overexpressed in neuronal cells. Eur J Neurosci 14:1678–1686.

Chemin J, Monteil A, Perez-Reyes E, Nargeot J, Lory P (2001c) The endogenous cannabinoid anandamide inhibits directly T-type Ca^{2+} channels. EMBO J 20:7033–7040.

Cribbs LL, Lee JH, Yang J, Satin J, Zhang Y, Daud A, Barclay J, Williamson MP, Fox M, Rees M, Perez-Reyes E (1998) Cloning and characterization of α_{1H} from human heart, a member of the T-type Ca^{2+} channel gene family. Circ Res 83:103–109.

Docherty RJ, Robbins J, Brown DA (1991) NG108-15 neuroblastoma X glioma hybrid cell line as a model neuronal system. In: Cellular neurobiology: a practical approach (Wheal H, Chad J, eds), pp 74–95. Oxford: IRL.

Fox AP, Nowycky MC, Tsien RW (1987) Single-channel recordings of three types of calcium channels in chick sensory neurones. J Physiol (Lond) 394:149–172.

Freedman SB, Dawson G, Villereal ML, Miller RJ (1984) Identification and characterization of voltage-sensitive calcium channels in neuronal clonal cell lines. J Neurosci 4:1453–1467.

Frischknecht F, Randall AD (1998) Voltage- and ligand-gated ion channels in floor plate neuroepithelia of the rat. Neuroscience 85:1135–1149.

Goshima Y, Ohsako S, Yamauchi T (1993) Overexpression of Ca^{2+}/calmodulin-dependent protein kinase II in Neuro2a and NG108–15 neuroblastoma cell lines promotes neurite outgrowth and growth cone motility. J Neurosci 13:559–567.

Gottmann K, Dietzel ID, Lux HD, Huck S, Rohrer H (1988) Development of inward currents in chick sensory and autonomic neuronal precursor cells in culture. J Neurosci 8:3722–3732.

Gu X, Spitzer NC (1997) Breaking the code: regulation of neuronal differentiation by spontaneous calcium transients. Dev Neurosci 19:33–41.

Hamprecht B, Glaser T, Reiser G, Bayer E, Propst F (1985) Culture and characteristics of hormone-responsive neuroblastoma × glioma hybrid cells. Methods Enzymol 109:316–341.

Han HQ, Nichols RA, Rubin MR, Bahler M, Greengard P (1991) Induction of formation of presynaptic terminals in neuroblastoma cells by synapsin IIb. Nature 349:697–700.

Higashida H, Yokoyama S, Hoshi N, Hashii M, Egorova A, Zhong ZG, Noda M, Shahidullah M, Taketo M, Knijnik R, Kimura Y, Takahashi H, Chen XL, Shin Y, Zhang JS (2001) Signal transduction from bradykinin, angiotensin, adrenergic and muscarinic receptors to effector enzymes, including ADP-ribosyl cyclase. J Biol Chem 382:23–30.

Kasai H, Neher E (1992) Dihydropyridine-sensitive and omega-conotoxin-sensitive calcium channels in a mammalian neuroblastoma-glioma cell line. J Physiol (Lond) 448:161–188.

Kleinman HK, Ogle RC, Cannon FB, Little CD, Sweeney TM, Luckenbill-Edds L (1988) Laminin receptors for neurite formation. Proc Natl Acad Sci USA 85:1282–1286.

Klugbauer N, Marais E, Lacinova L, Hofmann F (1999) A T-type calcium channel from mouse brain. Pflügers Arch 437:710–715.

Komeima K, Hayashi Y, Naito Y, Watanabe Y (2000) Inhibition of neuronal nitric-oxide synthase by calcium/calmodulin-dependent protein kinase IIα through Ser847 phosphorylation in NG108–15 neuronal cells. J Biol Chem 275:28139–28143.

Kushmerick C, Romano-Silva MA, Gomez MV, Prado MA (2001) Changes in Ca^{2+} channel expression upon differentiation of SN56 cholinergic cells. Brain Res 916:199–210.

Lautermilch NJ, Spitzer NC (2000) Regulation of calcineurin by growth cone calcium waves controls neurite extension. J Neurosci 20:315–325.

Lee JH, Daud AN, Cribbs LL, Lacerda AE, Pereverzev A, Klockner U, Schneider T, Perez-Reyes E (1999a) Cloning and expression of a novel member of the low voltage-activated T-type calcium channel family. J Neurosci 19:1912–1921.

Lee JH, Gomora JC, Cribbs LL, Perez-Reyes E (1999b) Nickel block of three cloned T-type calcium channels: low concentrations selectively block α_{1H}. Biophys J 77:3034–3042.

Lievano A, Bolden A, Horn R (1994) Calcium channels in excitable cells: divergent genotypic and phenotypic expression of alpha 1-subunits. Am J Physiol 267:411–424.

Lukyanetz EA (1998) Diversity and properties of calcium channel types in NG108–15 hybrid cells. Neuroscience 87:265–274.

Mariot P, Vanoverberghe K, Lalevee N, Rossier MF, Prevarskaya N

(2002) Overexpression of an alpha1H (Cav3.2) T-type calcium channel during neuroendocrine differentiation of human prostate cancer cells. J Biol Chem 277:10824–10833.

McCobb DP, Best PM, Beam KG (1989) Development alters the expression of calcium currents in chick limb motoneurons. Neuron 2:1633–1643.

McRory JE, Santi CM, Hamming KS, Mezeyova J, Sutton KG, Baillie DL, Stea A, Snutch TP (2001) Molecular and functional characterization of a family of rat brain T-type calcium channels. J Biol Chem 276:3999–4011.

Monteil A, Chemin J, Bourinet E, Mennessier G, Lory P, Nargeot J (2000a) Molecular and functional properties of the human α_{1G} subunit that forms T-type calcium channels. J Biol Chem 275:6090–6100.

Monteil A, Chemin J, Leuranguer V, Altier C, Mennessier G, Bourinet E, Lory P, Nargeot J (2000b) Specific properties of T-type calcium channels generated by the human α_{1I} subunit. J Biol Chem 275:16530–16535.

Mynlieff M, Beam KG (1992) Developmental expression of voltage-dependent calcium currents in identified mouse motoneurons. Dev Biol 152:407–410.

Newcomb R, Szoke B, Palma A, Wang G, Chen X, Hopkins W, Cong R, Miller J, Urge L, Tarczy-Hornoch K, Loo JA, Dooley DJ, Nadasdi L, Tsien RW, Lemos J, Miljanich G (1998) Selective peptide antagonist of the class E calcium channel from the venom of the tarantula *Hysterocrates gigas*. Biochemistry 37:15353–15362.

Nirenberg M, Wilson S, Higashida H, Rotter A, Krueger K, Busis N, Ray R, Kenimer JG, Adler M (1983) Modulation of synapse formation by cyclic adenosine monophosphate. Science 222:794–799.

Nowycky MC, Fox AP, Tsien RW (1985) Three types of neuronal calcium channel with different calcium agonist sensitivity. Nature 316:440–443.

Perez-Reyes E, Cribbs LL, Daud A, Lacerda AE, Barclay J, Williamson MP, Fox M, Rees M, Lee JH (1998) Molecular characterization of a neuronal low-voltage-activated T-type calcium channel. Nature 391:896–900.

Randall AD, Tsien RW (1997) Contrasting biophysical and pharmacological properties of T-type and R-type calcium channels. Neuropharmacology 36:879–893.

Sambrook JE, Fritsch EF, Maniatis T (1989) Preparation of radiolabeled DNA and RNA probes. In: Molecular cloning: a laboratory manual (Sambrook JE, Fritsch EF, Maniatis T, eds), pp 931–957. Cold Spring Harbor, NY: Cold Spring Harbor Laboratory.

Talley EM, Cribbs LL, Lee JH, Daud A, Perez-Reyes E, Bayliss DA (1999) Differential distribution of three members of a gene family encoding low voltage-activated (T-type) calcium channels. J Neurosci 19:1895–1911.

Taussig R, Sanchez S, Rifo M, Gilman AG, Belardetti F (1992) Inhibition of the omega-conotoxin-sensitive calcium current by distinct G proteins. Neuron 8:799–809.

Williams ME, Washburn MS, Hans M, Urrutia A, Brust PF, Prodanovich P, Harpold MM, Stauderman KA (1999) Structure and functional characterization of a novel human low-voltage activated calcium channel. J Neurochem 72:791–799.

Yaari Y, Hamon B, Lux HD (1987) Development of two types of calcium channels in cultured mammalian hippocampal neurons. Science 235:680–682.